ORIGINAL ARTICLE

On target selection as reflected by posterior ERP components in feature-guided visual search

Roberto Dell'Acqua[1,2] | **Mattia Doro[1]** | **Sabrina Brigadoi[1]** |
Brandi Lee Drisdelle[3] | **Amour Simal[4]** | **Valentina Baro[2,5]** | **Pierre Jolicœur[4]**

[1]Department of Developmental Psychology, University of Padova, Padova, Italy

[2]Padova Neuroscience Center, University of Padova, Padova, Italy

[3]Department of Psychological Sciences, Birkbeck University of London, London, UK

[4]Department of Psychology, Université de Montréal, Montreal, Quebec, Canada

[5]Department of Neuroscience, University of Padova, Padova, Italy

Correspondence
Roberto Dell'Acqua, Department of Developmental Psychology, University of Padova, Via Venezia, 8 35131 Padova, Italy.
Email: dar@unipd.it

Abstract

The N2pc event-related potential is a widely studied ERP component that reflects the covert deployment of visuo-spatial attention to target stimuli displayed laterally relative to fixation. Recently, an analogous ERP component, named N2pcb, has been proposed as a marker of the deployment of visuo-spatial attention to targets displayed on the vertical midline. Two studies that investigated the N2pcb component found analogous results, using however two different algorithms to compute the amplitude of N2pcb. One study subtracted the ipsilateral activity elicited by a lateral target from the bilateral activity elicited by a target displayed on the vertical midline, whereas the other study subtracted the bilateral activity elicited by target-absent displays from the bilateral activity elicited by a target displayed on the vertical midline. Here we show both algorithms estimate properly the N2pc as well as the N2pcb components. In addition, we explored whether the singleton detection positivity (SDP) component, a posterior bilateral positivity temporally concomitant to N2pc recently reported in studies using singleton search, could be observed in the present study in which a target was defined by a combination of features. Given that such component was indeed found using feature search, we named this component posterior processing positivity (PPP), and showed that bilateral activity elicited by target-absent displays is an adequate baseline for its correct isolation.

KEYWORDS
ERP, N2pc, PPP, visual search, visuo-spatial attention

1 | INTRODUCTION

The ERP method of analysis of EEG activity recorded from participants performing visual search tasks has become an important tool to track with millisecond precision the covert deployment of visuo-spatial attention to task-relevant (target) objects. The ERP component that has proved most informative in this field of study is N2pc (Eimer, 1996; Luck & Hillyard, 1994a, 1994b). When a to-be-selected target is displayed laterally relative to fixation, N2pc appears as a transient negativity usually unfolding from about 200 to 300 ms at parieto-occipital sites

---

contralateral to the visual hemifield in which the target is displayed.

The amplitude of N2pc is typically calculated as the difference between the ERP recorded at electrodes over the scalp contralateral to the visual field occupied by a lateral target and the ERP recorded at ipsilateral electrodes. This method assumes the ipsilateral ERP can serve as a control for the contralateral ERP. As such, N2pc is assumed to be unsuited to track the deployment of attention to a target displayed on the vertical midline intersecting the point of fixation (henceforth, midline target), because ipsilateral and contralateral are not defined for these retinal positions. However, visual receptive fields at or near the vertical midline project bilaterally to extrastriate regions of the visual cortex (Chen et al., 2022; Drew et al., 2014; Hubel & Wiesel, 1967; Nakamura et al., 2008; Papaioannou & Luck, 2020; Wandell et al., 2007; Zeki, 1993). This neuroanatomical consideration has recently led Doro et al. (2020) to look for evidence of attentional selection in the bilateral ERP elicited by midline targets. They used a visual search task in which a singleton target (a colored disk displayed among homogeneously gray disks) or a feature-defined target (a colored disk displayed among heterogeneously colored disks) were displayed either laterally or on the vertical midline. Detecting the presence of a target colored disk when displayed among homogeneously gray disks is typically faster than detecting it when displayed among heterogeneously colored disks (Bacon & Egeth, 1994; see also Feldmann-Wüstefeld & Schubö, 2015; Mazza et al., 2009). Given this difference in search time, Doro et al. (2020) predicted, and observed, a corresponding difference in the onset latency of N2pc for lateral targets across these search conditions. Midline targets elicited a bilateral (i.e., averaged over posterior symmetrical electrodes) negativity that was undistinguishable from the contralateral negativity elicited by lateral targets. This pattern of results suggested attentional selection of midline targets elicited a bilateral N2pc (or N2pcb; Doro et al., 2020). The onset of N2pcb for midline targets was delayed in feature search compared to singleton search to the same extent as the delay for N2pc for lateral targets, providing critical support for the hypothesized functional similarity between N2pc and N2pcb (Doro et al., 2020).

Further support for the similarity between N2pc and N2pcb was reported by Monnier et al. (2020), who showed that N2pc and N2pcb share an additional property. It is now well established that the amplitude of N2pc is substantially attenuated, and sometimes even reversed in polarity, for lateral targets displayed in the upper visual hemifield (i.e., above the horizontal midline intersecting the point of fixation) compared to lateral targets displayed in the lower visual hemifield (e.g., Bacigalupo & Luck, 2019; Luck et al., 1997; Monnier

et al., 2020). A likely explanation of this N2pc difference is that targets displayed in the lower visual hemifield project to more dorsal regions of the posterior cortex, whereas targets displayed in the upper visual hemifield project to more ventral regions of the posterior cortex. This difference in the cortical representation of targets could alter distance and angle of equivalent dipoles contributing visual ERPs, and are likely to affect amplitude and polarity of signals recorded at posterior electrodes. Using a visual search design in which a target color singleton had to be detected among homogeneously colored distractors, Monnier et al. (2020) observed an N2pc in the usual form when a lateral target was displayed in the lower visual hemifield, and a polarity reversal of N2pc when a lateral target was displayed in the upper visual hemifield. Interestingly, an identical pattern of results was observed for N2pcb when a midline target was displayed above or below the point of fixation, and this result was interpreted as suggesting that the similarity of N2pc and N2pcb was not simply at the functional level but also at the level of their neural sources.

Albeit similar in their conclusions, the approach taken by Doro et al. (2020) and by Monnier et al. (2020) for N2pcb amplitude estimation differed in one important respect. Doro et al. (2020) isolated the N2pcb by subtracting the ipsilateral ERP recorded on trials with a lateral target from the bilateral ERP recorded on trials with a midline target. To justify their choice, these authors noted that a number of manipulations of target attributes in visual search were reflected in amplitude variations of the contralateral ERP, with minimal-to-nil variations of the ipsilateral ERP, that could thus be used as an appropriate baseline for both N2pc and N2pcb amplitude calculation. The ipsilateral ERP was shown to be invariant to manipulations of target color (Luck et al., 2006), target versus non-target feature selection (Luck & Hillyard, 1994a), target position relative to the horizontal midline (Luck et al., 1997; Perron et al., 2009), target numerosity (Benavides-Varela et al., 2018; Mazza & Caramazza, 2011), and target selection difficulty (Luck et al., 1997). Monnier et al. (2020), on the other hand, isolated the N2pcb by subtracting the bilateral ERP recorded on target-absent trials from the bilateral ERP recorded on trials with a midline target. Monnier et al. (2020) justified their choice by showing that amplitude, latency, and scalp topography of N2pcb did not differ from those of N2pc when these ERP components were calculated by subtracting the bilateral target-absent ERP from either the contralateral ERP elicited by a lateral target (N2pc), or the bilateral ERP elicited by a midline target (N2pcb). This finding led Monnier et al. (2020) to suggest that the bilateral ERP recorded on target-absent trials could be used as an appropriate baseline for both N2pc and N2pcb amplitude calculation.

Given the lack of direct empirical evidence for the equivalence of the ipsilateral ERP on target-present trials with lateral targets and the bilateral ERP on target-absent trials using the same experimental design and same physical stimulation, one objective of the present study was to fill this gap by adapting the design employed by Monnier et al. (2020) so as to incorporate the search conditions tested by Doro et al. (2020). From an algorithmic perspective, we sought to determine whether the two baselines chosen by Doro et al. (2020) and Monnier et al. (2020) for N2pc/N2pcb calculation (i.e., ipsilateral ERP on trials with a lateral target and bilateral ERP on target-absent trials, respectively) were equivalent in the N2pc/N2pcb time-range across singleton and feature search. From a more conceptual perspective, we wondered whether the ipsilateral ERP recorded on target-present trials with a lateral target could be inflated by positive activity indexing the suppression of salient distractor(s) contained in the visual hemifield opposite the target (so-called distractor positivity, or P_D; Hickey et al., 2009). If, as is sometimes implicitly assumed, distractor suppression is at play *only* when a target is present in the opposite visual hemifield (e.g., Gaspar & McDonald, 2014; but see Drisdelle & Eimer, 2021), it is possible the baseline used by Doro et al. (2020) for N2pc/N2pcb amplitude calculation was generally more positive, due to a P_D, than the target-absent baseline chosen by Monnier et al. (2020). Using a design in which the ipsilateral ERP could be directly compared with ERPs elicited by a range of target-absent displays composed of distractors varying in salience, we could ascertain whether the N2pc/N2pcb activity was overestimated by Doro et al. (2020) in comparison to the N2pc/N2pcb activity reported by Monnier et al. (2020).

One thing that is sometimes (benignly) neglected in ERP studies of visual search is that the subtractive approach employed to isolate N2pc is entirely blind to bilateral activity concomitant with N2pc, because the contralateral minus ipsilateral subtraction cancels out such activity. This bilateral ERP activity can however be brought to the fore by adopting other forms of ERP subtraction, as was recently shown by Tay et al. (2019) in the context of singleton search. These authors presented monochromatic target-absent displays containing bars homogeneously oriented vertically or horizontally. On target-present displays, one of the bars was oriented perpendicularly to all others. Tay et al. (2019) explored an ERP component that emerged by comparing ipsilateral and contralateral ERPs to a lateral target after subtracting the bilateral ERP recorded on target-absent trials. Following the subtraction, the difference contralateral and ipsilateral ERPs recorded at the same electrodes as those used to detect the N2pc were characterized by a positive deflection,

termed singleton detection positivity (or SDP), that onset slightly before N2pc, at 200 ms, and offset at about 400 ms post-stimulus. Critically, the topographical distribution of the SDP was clearly distinct from the P3b pervasively observed following a successful detection of a searched target, with separable and symmetrical foci that were more laterally and occipitally located than the typical centro-parietal focus of the P3b. The SDP component was also reported by Tay et al. (2022), who employed a combination of singleton search and go/no-go tasks. Participants searched displays identical to those of Tay et al. (2019) that could however be composed of homogeneously cyan or yellow bars. For one of these colors (go trials), participants had to indicate whether the search display contained an orientation singleton or not via a rapid button press. For the other color, participants had to make no response (no-go trials). The SDP component, that as in the previous study (Tay et al., 2019) onset before N2pc and unfolded between 200 and 400 ms post-stimulus, had a larger amplitude in go trials than no-go trials, and this result provided a further empirical characterization of the SDP activity. Given that, so far, the SDP component has been explored only in singleton search, one question we sought to answer in the present study was whether a component with similar characteristics to SDP could be found in feature search, by adopting the same subtractive approach used by Tay et al. (2019, 2022). A critical question in the present study was related to the proposed dissociability of SDP from P3b, which we sought to answer by taking a different approach than a topographical comparison between these ERP components. In particular, we used an ICA approach (Makeig et al., 1997) to the analysis of ERPs (e.g., Dell'Acqua et al., 2015; Simal & Jolicœur, 2020) so as to test whether SDP-like activity could be detected in one or more ICA components with a time-course that was spatio-temporally independent of the P3b time-course.

2 | METHOD

2.1 | Participants

Nineteen students at the Université de Montréal (11 women, 8 men) took part in the experiment after giving informed consent. Their mean age was 24.4 years ($SD = 3.6$), and all had normal or corrected-to-normal visual acuity. Two participants were removed from the final sample, one due to less than 60% correct responses in the visual search task, and the other due to more than 30% EEG epochs contaminated by eyeblinks and other EEG artifacts. The final sample included seventeen participants. The experimental protocol was vetted by the local Ethical Committee.

2.2 | Stimuli and procedure

The experiment was conducted using the multiple frame procedure (MFP; Aubin & Jolicœur, 2016) illustrated in Figure 1. Equiluminant stimuli (9.2 cd/m²) were presented against the black background of a 17-inch CRT monitor, at a viewing distance of about 57 cm. Twelve circles with a radius of 0.5° of visual angle were displayed evenly spaced along a notional circle with a radius of 3.5° of visual angle, centered at fixation. Each circle contained a gray tilted bar. A target was defined at the beginning of the experiment—and was kept fixed throughout the entire experiment for a given participant—as a specific combination of circle color and bar orientation, as shown in the upper left corner of Figure 1. The possible colors were

blue (RGB = 0, 110, 255), green (RGB = 53, 134, 0), fuchsia (RGB = 245, 0, 110), violet (RGB = 195, 59, 239), and dark orange (RGB = 206, 104, 0). The possible bar orientations were ±5° relative to the vertical. All combinations of target color and bar orientation were used in the experiment, counterbalanced across participants.

In the present design, frames could be classified according to whether they contained only a circle in the target color (feature-present frames; e.g., a green circle including a bar whose orientation did not match the target orientation; as in frame F6 in Figure 1), a target proper (target-present frames; e.g., a green circle including a bar whose orientation matched the target orientation; as in frames F1 and F3 in Figure 1), or neither of these features (target-absent frames). In both feature-present and
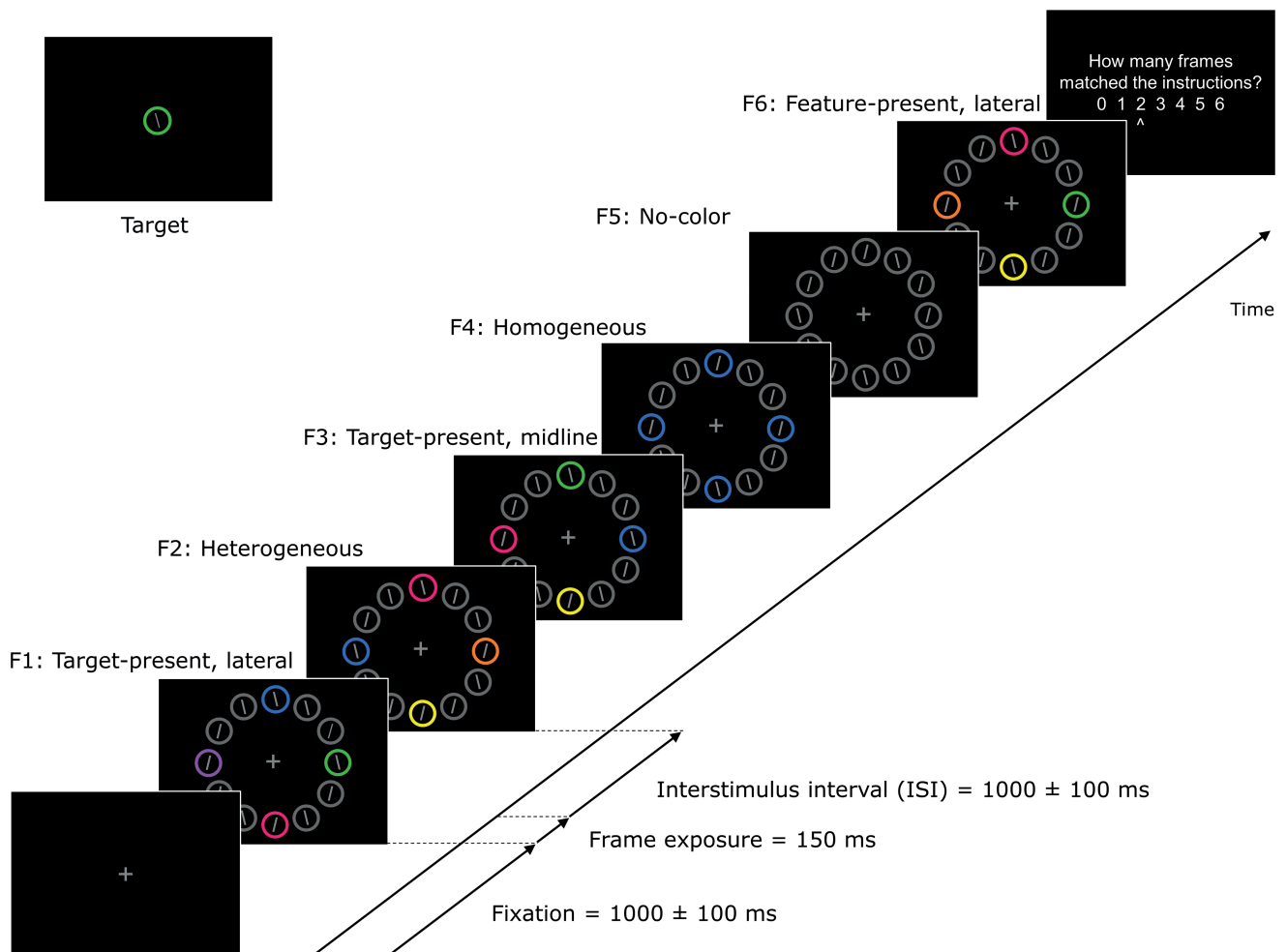

FIGURE 1 Example of a 6-frame MFP trial. A target circle (e.g., a green circle containing a bar in a specific orientation, as in the top left frame) could be displayed in a lateral position (3 or 9 o'clock) or in a midline position (12 or 6 o'clock). When a frame contained a circle in the target color, the bar inside this circle could be oriented as a target (target-present frame; as in frames F1 and F3) or a non-target (feature-present frame, as in frame F6). To avoid clutter, the blank frames interposed between each two successive frames in the actual experiment have been omitted in this figure. The size of the stimuli is approximately to scale with the stimuli as displayed on the computer monitor used in the experiment. Hue and brightness of the stimuli have been chosen so as to maximize clarity of the depiction, and are only partially faithful to the stimuli used in the experiment (see Section 2.2 for the correct values).

target-present frames, the circle in the target color could appear with equal probability in one of four possible positions, namely, 12 or 6 o'clock positions (midline positions), or 3 or 9 o'clock (lateral positions). In both feature-present and target-present frames, the circle in the target color was always accompanied by three heterogeneously colored circles displayed at the three other possible positions and by eight circles colored in gray (RGB = 140, 140, 140). Target-absent frames could be further subdivided according to whether the four circles displayed at midline and lateral positions were heterogeneously colored (heterogeneous condition, as in frame F2 in Figure 1), homogeneously colored in a non-target color (homogeneous condition, as in frame F4 in Figure 1), or of the same gray color as the circles in the remaining positions (no-color condition, as in frame F5 in Figure 1).

Each trial consisted of 6 consecutive frames, each presented for 150 ms with a blank inter-stimulus interval (ISI) of 1000 ± 100 ms, allowing enough time to ensure that perceptual and cognitive processes deployed for each frame would not cause interference with trailing and/or preceding frames (e.g., Crebolder et al., 2002). Participants initiated each trial by pressing the spacebar of the keyboard of the PC controlling stimulus presentation and EEG synchronization. The first frame was presented 1000 ± 100 ms following the spacebar press. At the end of each 6-frame trial, participants had to indicate, with no speed pressure, the number of target-present frames (i.e., the number of frames including the target combination of circle color and bar orientation defined at the beginning of the experiment), by moving a cursor left or right, using the arrow keys of the keyboard (as shown in the last frame in Figure 1). After the response, feedback on accuracy was provided by presenting two digits at the center of the screen separated by a slash. The digit on the left was the participant's response, and the one on the right was the correct response.

A total of 1428 frames (238 experimental 6-frame trials) were presented to each participant, 816 of which included a circle in the target color in a midline or lateral position (204 frames per position). Half of these frames were feature-present frames whereas the other half were target-present frames. Of the 612 target-absent frames, 204 were homogeneous frames, 204 were heterogeneous frames, and 204 were no-color frames.

2.3 | EEG/ERP recordings and analysis

EEG activity was recorded at a sampling frequency of 512 Hz using a BioSemi Active Two system and an elastic cap with 64 Ag/AgCl electrodes positioned according to the International 10/10 system (Sharbrough et al., 1991),

at sites Fp1, Fpz, Fp2, AF7, AF3, AFz, AF4, AF8, F7, F5, F4, F1, Fz, F2, F4, F6, F8, FT7, FC5, FC3, FC1, FCz, FC2, FC4, FC6, FT8, T7, C5, C3, C1, Cz, C2, C4, C6, T8, TP7, CP5, CP3, CP1, CPz, CP2, CP4, CP6, TP8, P9, P7, P5, P3, P1, Pz, P2, P4, P6, P8, P10, PO7, PO3, POz, PO4, PO8, O1, Oz, O2 and Iz. HEOG activity was recorded from electrodes positioned at the outer canthi of both eyes. VEOG activity was recorded from an electrode placed below the left eye and from Fp1. Impedance at each electrode site was maintained below 10 KΩ. EEG, HEOG, and VEOG activities were re-referenced offline to the average of the left and right mastoids. EEG activity was then segmented into 1100 ms epochs starting 100 ms before the onset of each frame and ending 1000 ms after. Epochs were baseline corrected using the mean activity in the −100 to 0 ms interval. Epochs were rejected based on the presence of artifacts (i.e., VEOG deflections greater than 50 μV within a time-window of 150 ms, HEOG deflections greater than 35 μV within a time-window of 300 ms, or EEG signal exceeding ±100 μV anywhere in the epoch in the remaining channels).

3 | RESULTS

3.1 | Behavior

Given the use of the MFP paradigm, it was not possible to isolate response accuracy on a per-frame basis. The overall mean proportion of correct responses (i.e., when participants reported the correct number of frames containing a target at the end of the frame sequence) was .89 ($SD = .07$). Because a correct count was the result of six consecutive correct decisions, to a first approximation (e.g., ignoring canceling errors, which had a negligible probability in the present case), the probability of a correct decision for each frame was about the sixth root of the mean proportion of correct responses, or .98.

3.2 | ERPs (N2pc and N2pcb)

Figure 2 shows ERPs elicited by feature-present and target-present frames displayed laterally or on the vertical midline, and ERPs elicited by the three types of target-absent frames used in the present experiment.

Given the non-orthogonality of the experimental design, individual mean ERP amplitudes in the time-window of interest (i.e., 200–300 ms, marked by the rectangular dashed outline in Figure 2) were submitted to two separate repeated-measures ANOVAs. The first ANOVA examined conditions where a circle in the target color was present by considering frame type (2 levels: target-present
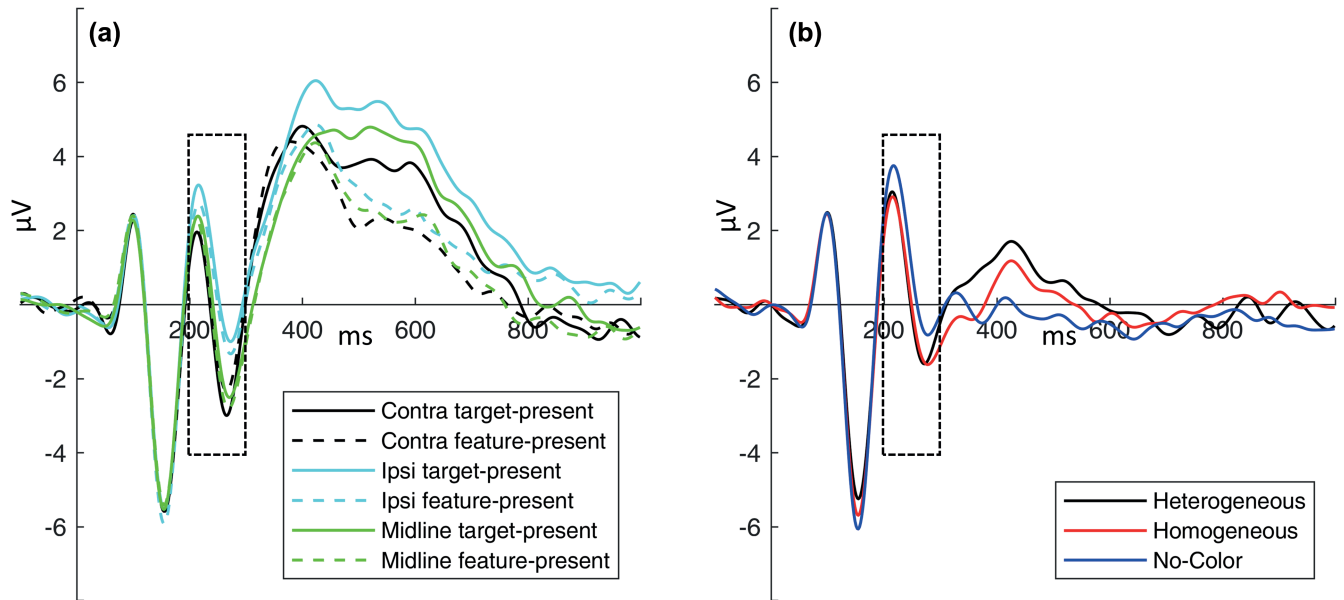
FIGURE 2 ERPs elicited at PO7/PO8 electrodes. (Panel a) ERPs elicited by target-present (solid lines) and feature-present (dashed line) frames. (Panel b) ERPs elicited by target-absent frames. The dashed rectangle in each graph indicates the time-window for ERP amplitude analysis. Positive voltage is plotted upward. Contra = contralateral; Ipsi = ipsilateral.

vs. feature-present) and circle/electrode relative position (3 levels: contralateral to a lateral circle vs. ipsilateral to a lateral circle vs. bilateral to a midline circle) as within-subject factors. The ANOVA indicated that ERPs recorded in the 200–300 ms time-window did not differ between target-present and feature-present frames ($F[1, 16] = 0.3$, $p = .583$). For target-present and feature-present frames, ERPs were however significantly influenced by the position of the circle in the target color ($F[2, 32] = 33.5$, $\eta_p^2 = .488$, $p < .001$). FDR corrected (Benjamini & Hochberg, 1995) t tests indicated that, the amplitude of the ERP contralateral to a lateral circle ($M = -0.44 \mu V$) and the amplitude of the bilateral ERP to a midline circle ($M = -0.43 \mu V$) were not significantly different ($t[16] = -0.1$, $p = .960$). However, the ipsilateral ERP to a lateral circle ($M = 0.74 \mu V$) was more positive than the contralateral ERP ($t[16] = 5.2$, $p < .001$), and more positive than the bilateral ERP to a midline circle ($t[16] = 4.3$, $p < .001$). A series of FDR corrected t tests confirmed the statistical equivalence of ERPs elicited by target-present and feature-present frames in each of the circle possible positions (max $t[16] < -1.7$, min $p > .22$). Based on these results, the factor frame type (target-present vs. feature-present) was no longer considered in subsequent analyses, and the corresponding ERP values averaged over these two frame types.

The second ANOVA examined ERPs in the 200–300 ms time-window elicited by target-absent frames, that is, by frames that did not include a circle in the target color, by considering distractor type (3 levels: heterogeneous vs. homogeneous vs. no-color) as a within-subject factor. The ANOVA detected a significant effect of distractor type

($F[2, 32] = 5.3$, $\eta_p^2 = .248$, $p = .010$). FDR corrected t tests showed that the bilateral ERP for no-color frames (1.2 μV) was more positive than ERPs for both heterogeneous frames (0.4 μV; $t[16] = 2.5$, $p = .039$) and homogeneous frames (0.3 μV; $t[16] = 2.6$, $p = .039$), which did not differ from each other ($t[16] = 0.3$, $p = .743$).

A complementary series of t tests was carried out to detect all possible statistical differences that were not investigated in the previous analyses because of the lack of orthogonality of the design (i.e., each condition including a circle in the target color vs. each target-absent condition). The results are summarized in Table 1. Critically, these comparisons revealed no significant difference between the ipsilateral ERP to a laterally displayed circle in the target color and ERPs in all other target-absent conditions.

One anticipated objective of the present study was to evaluate the hypothetical equivalence between ERP activity recorded under target-absent conditions and the ipsilateral ERP elicited by a lateral target. Because this is an expected null-finding, we supplemented the series of t tests reported above with Bayes factor calculations. We computed Bf_{01} for all three comparisons, indicating the likelihood of the null hypothesis using a Cauchy distribution as prior with $\sqrt{2}/2$ scale (Morey & Rouder, 2011). Converging with the results of the t tests, the Bayesian analysis suggested positive evidence for the null hypothesis. That is, the ipsilateral ERP elicited by lateral targets was unlikely to be different from the bilateral ERPs elicited by heterogeneous frames ($Bf_{01} = 3.3$), homogeneous frames ($Bf_{01} = 2.8$), and no-color frames ($Bf_{01} = 3.9$).

Figure 3 shows difference ERPs obtained by subtracting the ipsilateral ERP elicited by frames including a laterally displayed circle in the target color and bilateral ERPs

TABLE 1 Results of the pair-wise comparisons by *t* test, with FDR corrected *p* values, of mean ERP amplitude recorded in a 200–300 ms time-window from frames that contained a circle in the target color (feature-present and target-present frames) crossed with the three target-absent frames (heterogeneous, homogeneous, and no-color frames)

	t(16)	*p*
Contralateral versus heterogeneous	−3.2	.005
Contralateral versus homogeneous	−2.3	.033
Contralateral versus no-color	−3.8	.001
Ipsilateral versus heterogeneous	1.3	.211
Ipsilateral versus homogeneous	1.4	.171
Ipsilateral versus no-color	−1.1	.267
Midline versus heterogeneous	−3.5	.002
Midline versus homogeneous	−2.1	.052
Midline versus no-color	−3.8	.002

elicited by the three different target-absent frames from contralateral and midline ERPs elicited by (averaged) feature-present and target-present frames.

Given the reinstatement of design orthogonality after collapsing ERP activity in feature-present and target-present frames, a final ANOVA was carried out on N2pc and N2pcb amplitude estimated in a 200–300 ms time-window to inspect whether these components differed when calculated using the different baseline ERPs implemented in the present paradigm. The ANOVA considered component (2 levels: N2pc vs. N2pcb) and baseline (4 levels: ipsilateral vs. heterogeneous vs. homogeneous vs. no-color) as within-subject factors. The ANOVA indicated a significant effect of baseline ($F[3, 48] = 3.3$, $\eta_p^2 = .115$, $p = .027$), and neither effect of component ($F[1, 16] = 0.2$, $p = .898$) nor of the interaction between these factors ($F[1, 16] = 0.8$, $p = .522$). A series of FDR corrected *t* tests showed N2pc/N2pcb amplitude did not differ when calculated using as baseline the ERP elicited by heterogeneous frames (−1.0 µV), homogeneous frames (−0.9 µV), and
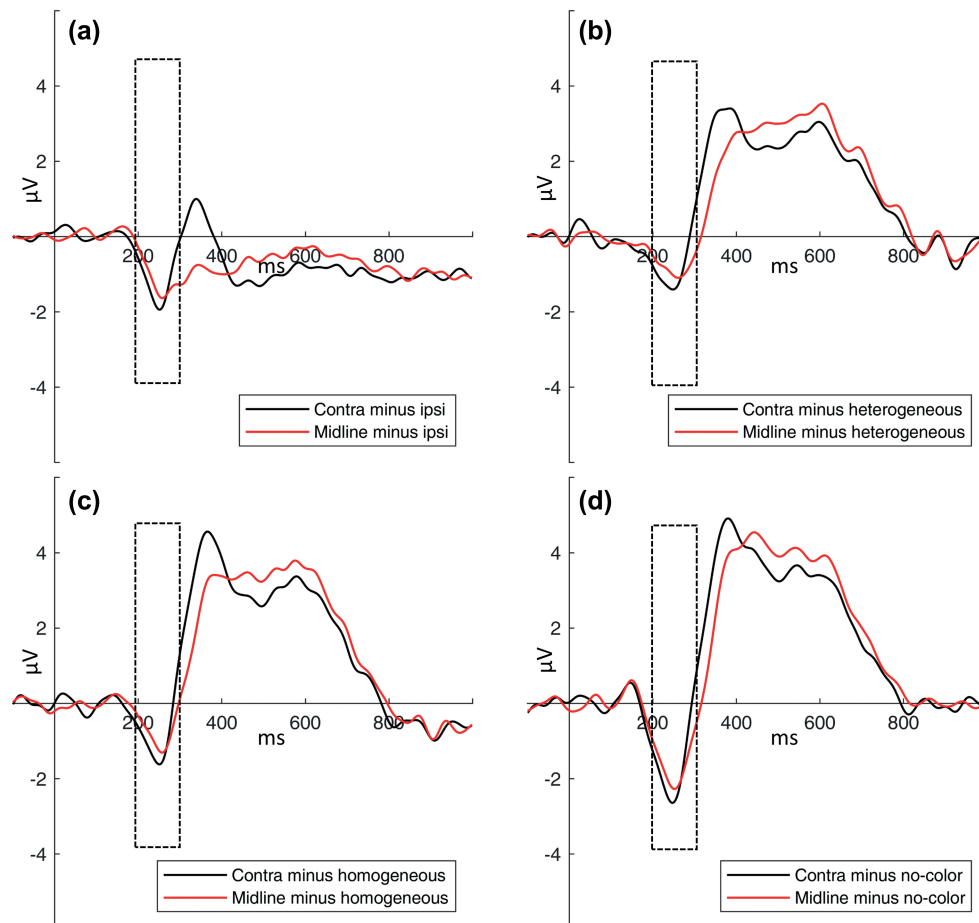
FIGURE 3 Difference in ERPs recorded at PO7/PO8 generated by treating as baselines for N2pc/N2pcb amplitude calculation the ERP ipsilateral to a circle in the target color (Panel a), the bilateral ERP elicited by heterogeneous frames (Panel b), homogeneous frames (Panel c), and no-color frames (Panel d). Dashed rectangles in the graphs indicate the time-window for N2pc/N2pcb amplitude analysis. Positive voltage is plotted upward. Contra = contralateral; Ipsi = ipsilateral.

no-color frames (-1.7 µV) (max $t = 2.6$, min $p = .072$). No other comparison was significant (max $t = 1.4$, min $p = .304$).

Incidentally, the difference ERPs plotted in Panel (a) of Figure 3, where N2pc and N2pcb were generated using the prototypical subtraction with ipsilateral ERPs as a common baseline for contralateral and midline ERPs, showed a pattern analogous to that recently observed by Chen et al. (2022) in a study describing a bilateral SPCN (Jolicœur et al., 2006; or CDA, Vogel & Machizawa, 2004; i.e., a contralateral negativity usually trailing N2pc in visual working memory tasks) as a reflection of memory maintenance of visual memoranda displayed on the vertical midline. More specifically, whereas N2pc and SPCN for lateral visual memoranda were separated by an evident return to the 0 baseline interposed between these components, N2pcb and SPCNb for midline visual memoranda tended to overlap, and appeared as a monophasic negative deflection with no clear components' interruption. A pattern resembling that observed by Chen et al. (2022) is evident in Panel (a) of Figure 3, in that N2pcb (red waveform), contrary to N2pc (black waveform), appeared as a monophasic negativity increase blending N2pcb and SPCNb. We speculated this difference could be ascribed to retinotopy and the bilateral cortical representation of midline targets (Chen et al., 2022; Doro et al., 2020; Monnier et al., 2020) versus the unilateral (and more eccentric) representation of lateral targets, although it is only with further work that an empirically grounded explanation for this intriguing difference could be found. For now, we noted that, when ERPs elicited by bilaterally represented distractors contained in target-absent frames were subtracted from

contralateral and bilateral target-elicited ERPs, this particular difference between N2pc and N2pcb was no longer evident, as shown in Panels (b–d) of Figure 3.

3.3 | ICA of ERPs (posterior processing positivity, or PPP)

Figure 4 contains the difference target-present minus target-absent ERPs corresponding to those used by Tay et al. (2019, 2022) for the isolation of the SDP component. To reiterate its most distinguishing features, SDP in Tay's et al. (2019, 2022) singleton search studies had an onset about 200 ms post-stimulus, shortly before the N2pc onset, and an offset about 400 ms post-stimulus.

Figure 4 makes clear that a prominent positive ERP deflection was also found in the present context, as a result of the subtraction of target-present minus target-absent ERPs, with a time-course and topographical distribution that were however substantially different from those of SDP. Given the different nature of the target and search mode employed in the present context *vis-à-vis* Tay et al.'s singleton search, we named this component posterior processing positivity, or PPP. The present PPP component had an onset about 300 ms post-stimulus, seemingly coinciding with the offset of N2pc, and an offset about 800 ms post-stimulus. Topographically, the PPP had a distribution that was not bi-focal as the SDP, and not symmetrical, with a focus that was spatially closer to ipsilateral electrodes, that were positioned on the right of the scalp reported in Panel (b) of Figure 4. We suspected this intertwined pattern of ERPs to be a complex
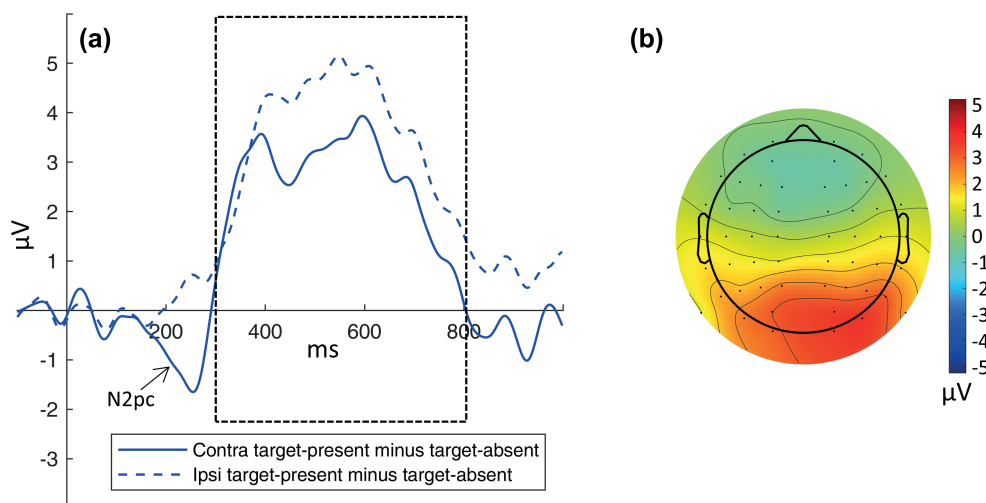
FIGURE 4 (Panel a) ERPs elicited at PO7/PO8 generated by subtracting the bilateral ERP elicited by target-absent heterogeneous frames from contralateral and ipsilateral ERPs elicited by target-present frames (i.e., frames including the target combination of colored circle and bar orientation). Positive voltage is plotted upward. Contra = contralateral; Ipsi = ipsilateral. (Panel b) Top-viewed topographic map of difference ERPs in a 300–800 ms time-window, indicated by the dashed rectangle in Panel (a), with contralateral and ipsilateral electrodes positioned over the left and right sides of the scalp, respectively.

spatio-temporal mixture of several cortical sources contributing ERP activity. Although the EEG reflection of some of these sources could ostensibly be isolated at the scalp level with subtraction approaches, it is important to note subtractions can sometimes miss or hide effects (e.g., bilateral influences canceled out by contralateral vs. ipsilateral comparisons) or make it impossible to observe some effects (e.g., for midline stimuli). Critically for the present context, it was practically impossible to discern whether the asymmetrical scalp distribution of PPP, characterized by a spatial imbalance in the peak towards ipsilateral electrodes, was an intrinsic property of PPP or instead resulted from the intrusion of SPCN/CDA to a more symmetric and bilateral PPP, yielding an apparent net ipsilateral positivity increment determining the asymmetrical topography shown in Panel (b) of Figure 4.

The solution to ERP components' spatio-temporal overlap adopted in the present context was to submit ERPs to ICA decomposition using the algorithm implemented in EEGLAB (Delorme & Makeig, 2004). The results of an ICA decomposition are temporally independent sources of the whole activity recorded over the scalp as EEG/ERP signal. Each independent component has two aspects. One aspect is a time invariant topographical scalp distribution and the other aspect is an associated activation waveform that varies over time. Succinctly, the original ERP data can be reconstructed by multiplying the values represented in the temporally fixed scalp plots by the momentary amplitude of the activation time-course for each independent component, and summing these values over all the components in the analysis. This method has been successfully used with ERPs in the past to unmix the different spatio-temporal dynamics of underlying activity (e.g., Dell'Acqua et al., 2015; Simal & Jolicœur, 2020; see also Dien & Frishkoff, 2005, for a detailed discussion of a similar approach). In the present context, the analysis was performed considering the ERPs of each participant for the eleven primary experimental conditions, that is, the conditions containing a circle in the target color (8 levels; 4 positions: up, down, left, right ×2 frame types: target-present, feature-present) and the target-absent conditions (3 levels: heterogeneous vs. homogeneous vs. no-color). ERPs were initially analyzed using singular value decomposition to determine the dimensionality of the signal subspace containing most of the relevant event-related activity. A screen plot of the singular values showed a clear break after the first six components. The ICA analysis was thus restricted to this subspace of the signal. From the first to the sixth component, ICA components are referred to as ICA-1, ICA-2, ICA-3, ICA-4, ICA-5, and ICA-6 in the forthcoming.

We first focused on independent components that underlay lateralized activity, and were therefore unlikely sources of a bilaterally expected sign of PPP activity germane to SDP. To do this, we considered the differential activity elicited by frames containing a circle in the target color (i.e., averaged over feature-present and target-present frames) presented on the left visual hemifield minus the activity elicited by a circle in the target color presented on the right visual hemifield in a 200–300 ms time-window for each component, and compared these activities against 0 with FDR corrected t tests. The results showed that ICA-3 and ICA-6 were both significantly different from 0, indicating a lateralization effect ($t[16] = -3.7$, $p = .003$ and $t[16] = 3.5$, $p = .003$, respectively). Scalp topography and time-course of ICA-3 and ICA-6 are illustrated in Figure 5.

The scalp distribution for ICA-3 captures the relative contralateral negativity elicited by frames containing a circle in the target color in the right visual field. The associated subtraction waveform shows what appears as a typical N2pc in the 200–300 ms window. ICA-6 scalp distribution captures the complementary scalp plot associated with frames containing a circle in the target color in right visual field, and associated N2pc. Further, we examined whether ICA-3 and ICA-6, in addition to N2pc, also contained a SPCN reflecting the engagement of visual working memory. We focused on target-present frames (i.e., frames including a target combination of colored circle and bar orientation), for which representations of the selected stimulus would be expected to be maintained in visual working memory (for counting purposes, as requested in the MFP procedure). The SPCN, estimated in a 400–900 ms time-window, was significantly different from 0 for both ICA-3 ($t[16] = 2.4$, $p = .027$) and ICA-6 ($t[16] = 3.4$, $p = .004$).

We then examined non-lateralized activations associated with frames including a circle in the target color (target-present and feature-present frames) for the remnant four components, namely, ICA-1, ICA-2, ICA-4, and ICA-5. Given the main effect of circle position and the interaction between circle position and frame type were not significant in a 400–1000 ms time-window ($F[3, 48] = 0.2$, $p = .901$ and $F[3, 48] = 0.9$, $p = .468$, respectively), we averaged these trials over circle positions in subsequent analyses. After subtracting activity elicited by target-absent heterogeneous frames, the scalp distributions and corresponding ICA time-courses are shown in Figure 6.

We evaluated the differences between target-present and feature-present ICA time-courses by means of FDR corrected t tests at each time-point throughout the duration of the whole epoch. Only clusters of time-points with at least 10 ms of duration were considered statistically significant and reported. The results are reported as a cyan bar along the x-axis of each time-course graphed in Figure 6. ICA-1 presented a parietal distribution reminiscent of P3b, and a time-window in which the
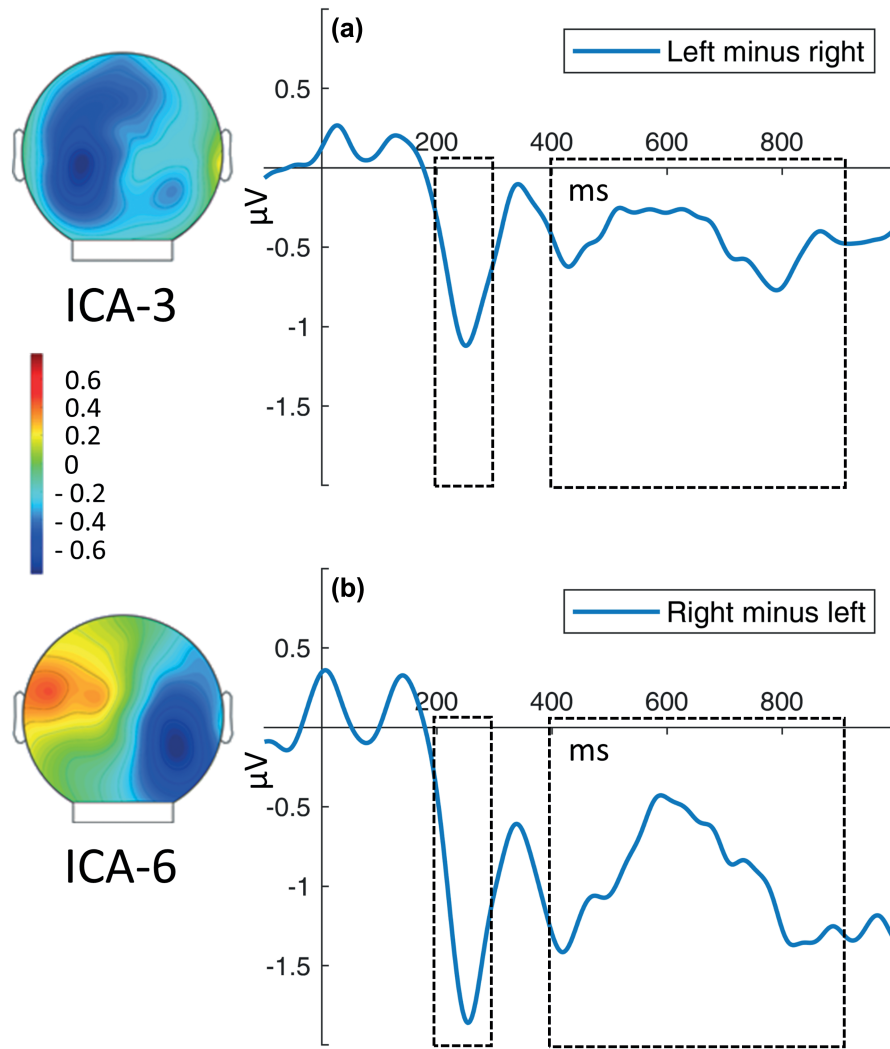
FIGURE 5 Results of the ICA analysis of ERPs. Back-viewed topographic maps (left) and corresponding time-courses of the ICA components (right) with a lateralized source generated by subtracting from the average time-course elicited by frames with a circle in the target color displayed in the left visual hemifield those displayed in the right visual hemifield (Panel a) and vice versa (Panel b). The dashed rectangles indicate the time-windows explored for the isolation of ICA components with a likely lateralized origin (i.e., N2pc and SPCN). Positive voltage is plotted upward.

target-present time-course was more positive than the feature-present time-course. ICA-2 had a more posterior scalp distribution that included Oz, and showed a pattern of difference between target-present and feature-present time-courses in a time-range similar to ICA-1. ICA-4 differed from the previous components in that it displayed a more complex spatial distribution, with a polar occipital focus and bilateral lateral foci. The ICA-4 component showed an increased amplitude for target-present relative to feature-present waveforms in a later time-window. ICA-5 presented a bilateral occipital activation peaking near PO7 and PO8, that is, it overlapped with N2pc. Given the bilateral and symmetrical occipital foci location, ICA-5 was probably the ICA component with the highest degree of resemblance to Tay's et al. (2019, 2022) SDP. The ICA-5 time-course showed however a different pattern compared

to SDP and to all other ICA components for, in three short time-windows included in the 200–400 ms time-range, the amplitude of the feature-present time-course was more positive than the amplitude of the target-present time-course, which reversed in a subsequent time-window.

To characterize the timing of the initial rise in positivity for these ICA components, we averaged over target-present and feature-present activations and estimated onset latency of each component using a jackknife approach (Kiesel et al., 2008) as the time-point at which individual jackknife waveforms reached 15% of the peak amplitude of the grand average. Jackknife scores were back-converted to individual participants' estimates using the method described in Brisson and Jolicœur (2008) and Smulders (2010). The mean onset latency was 427 ms for ICA-1, 302 ms for ICA-2, 425 ms
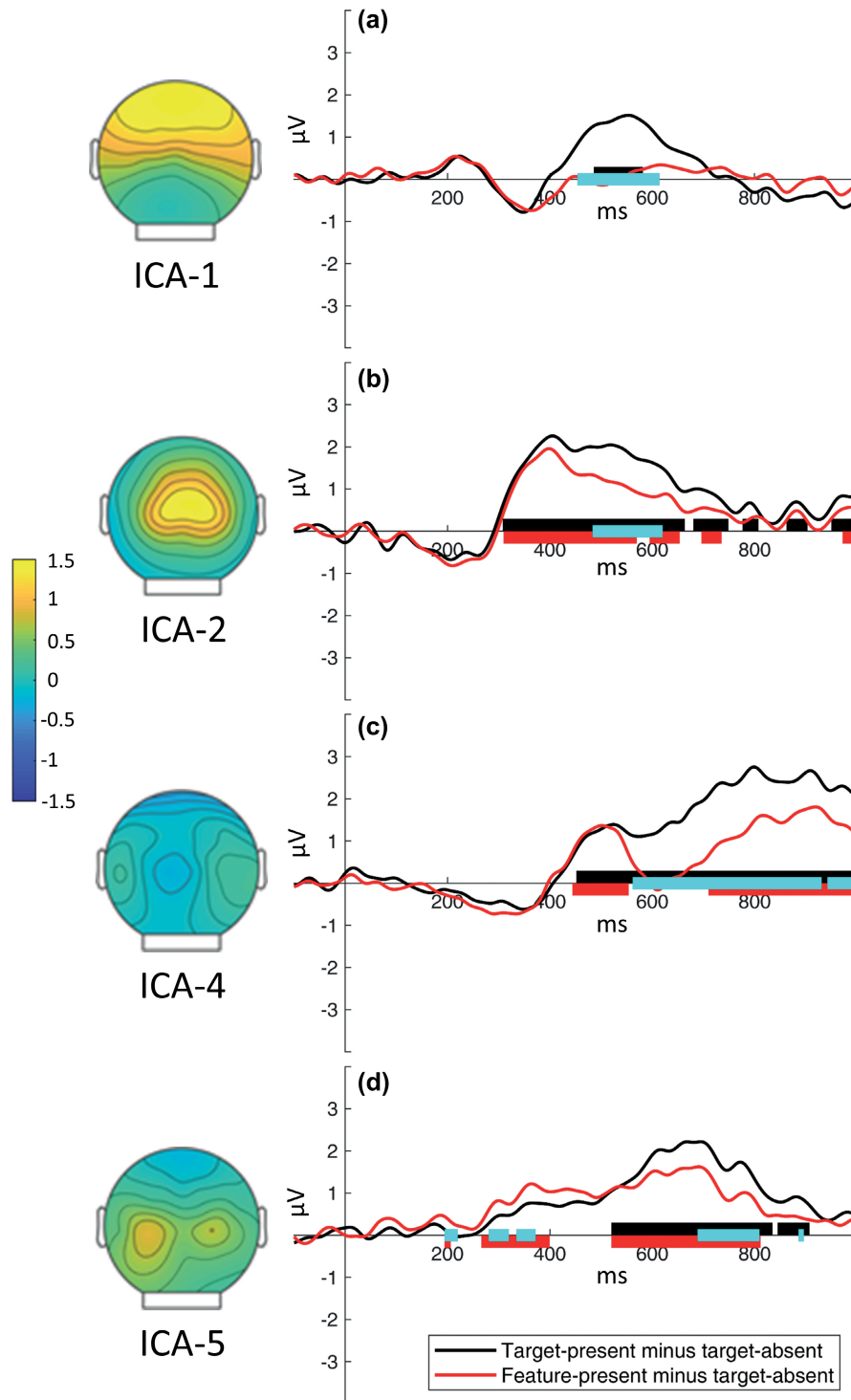
FIGURE 6 Results of the ICA analysis of ERPs. Back-viewed topographic maps (left) and corresponding time-courses of the ICA components generated by subtracting the time-course elicited by target-absent heterogeneous frames from the time-courses elicited by target-present and feature-present frames. Black and red lines displayed along the x-axis of the graphs on the right indicate a significant difference from 0 of the positive portion of the ICA time-courses displayed in the corresponding color, while cyan lines indicate a significant difference between target-present and feature-present time-courses in the indicated time-range. Positive voltage is plotted upward.

for ICA-4, and 271 ms for ICA-5. Individual latency estimates were submitted to an ANOVA with ICA components (4 levels: ICA-1 vs. ICA-2 vs. ICA-4 vs. ICA-5) as a within-subjects factor that confirmed these onset latencies were indeed different (F[3, 48 = 13.4, $\eta_p^2 = 0.455$, $p < .001$). FDR corrected t tests indicated ICA-5 onset earlier than ICA-2 (t[16] = 5.1, $p = .004$), both ICA-5 and ICA-2 onset earlier than ICA-1 and

ICA-4 (min $t[16] = 5.9$, max $p = .003$), and these latter did not differ from each other ($t[16] = 0.8$, $p = .960$).

Finally, in light of the earlier onset of SDP relative to N2pc observed by Tay et al. (2019, 2022) in singleton search, we explored the relative temporal distribution of N2pc and PPP in the present study. We compared the onset latencies of ICA-1, ICA-2, ICA-4, and ICA-5, with the onset latency of N2pc. N2pc onset latency was estimated by considering the ERPs shown in Figure 2[1] and using the latency of jackknifed activations at 15% of peak amplitude. The mean N2pc onset latency was 186 ms. Relative to N2pc onset, ICA-1, ICA-2, ICA-4, and ICA-5 onset significantly later (min $t[16] = 11.3$, $p < .001$ in all cases).

When collectively taken, these four components provided information about the late, most likely post-attentive, processing of task-relevant information, suggesting that the presence of a single feature of the target (i.e., the color of the circle) led to a positive-going activation starting about 300 ms post-stimulus for ICA-2, and between 400 ms and 500 ms for ICA-1 and ICA-4. Some peculiarities apart, the target-present and feature-present time-courses began to differ also in ICA-5, similarly to ICA-1 and ICA-4, with the target-present time-course showing a larger positivity than the feature-present time-course.

4 | DISCUSSION

Previous work had suggested the N2pcb is the bilateral equivalent to the N2pc, a marker of attentional deployment to a lateral target (Doro et al., 2020; Monnier et al., 2020). While both Doro et al. (2020) and Monnier et al. (2020) presented results supporting similar underlying mechanisms for both components, different "baselines" were used to isolate N2pcb, with Doro et al. (2020) using ipsilateral ERPs to lateral targets and Monnier et al. (2020) using bilateral ERPs from target-absent displays. One goal of the present investigation was therefore to provide direct evidence for an equivalence between these two baselines by comparing both difference calculations using a repeated-measures design, which would in turn support the functional equivalence between the N2pc and N2pcb claimed by Doro et al. (2020) and Monnier et al. (2020). Our results revealed no significant difference between

ipsilateral ERPs to a lateral target and bilateral ERPs from all three target-absent displays (heterogeneous, homogeneous, and no-color displays), supporting an equivalence between the target-present ipsilateral baseline and the entire range of target-absent baselines generated and tested in the present design. This result was supported by a Bayesian analysis that suggested the claimed equivalence between ipsilateral and target-absent baselines was plausibly true.

As alluded to in the Introduction, researchers in this field might have expected the ipsilateral ERP on target-present trials to show signs of distractor suppression in the N2pc/N2pc time-range in the form of a P_D component (e.g., Gaspar et al., 2016; Hickey et al., 2009; Jannati et al., 2013), especially in trials with a lateral target. The present results however showed that the ipsilateral ERP on target-present or feature-present trials was not more positive than the "baseline" bilateral ERPs recorded on target-absent trials. One inference that this particular result seems to legitimate is that distractor suppression was not necessary (and, thus, a P_D not elicited) in any conditions of the present experimental design, and irrespective of the presence of a target or a target-like feature in search frames. Perhaps this result is not surprising in light of ERP findings suggesting that distractors fail to elicit any type of ERP activity when participants search consistently for the same target throughout a visual search experiment, which was in fact the case for the participants in the present experiment (Jannati et al., 2013; Kiss et al., 2012; Sawaki & Luck, 2010). Moreover, the positions occupied by distractors in the present design were largely predictable, as distractors were displayed only in the two midline positions and the two lateral positions horizontally aligned with the fixation point. Spatial predictability is another factor that was shown to reduce the impact of distractors in visual search (Van Moorselaar & Slagter, 2019, 2020). Another possible reason a P_D was not observed in the present context can be inferred from studies focusing on variations of the ipsilateral ERPs during visual WM maintenance. These studies (e.g., Arend & Zimmer, 2011; Feldmann-Wüstefeld & Vogel, 2019) consistently showed that ERPs ipsilateral to to-be-encoded lateral visual memoranda were affected by distractors only when visual WM load was minimal (e.g., load of one to-be-encoded single-feature object, but not two). The hypothesis in those cases was that distractors intrude and impact visual WM maintenance because the minimal load leaves unused "slots" that can be occupied by distractors (Lavie et al., 2004, 2014). In this vein, it must be noted that search in the present design was accomplished for a particularly "slot-consuming" target, that was defined

---

[1] N2pc onset latencies were similar across ERPs and lateralized ICA-3/ICA-6, and positively correlated ($r = .77$, $p < .001$). When performed on N2pc onset latency values derived from ICA-3/ICA-6 time-courses, the results of the present analysis of N2pc latency values derived from ERPs did not change.

by a conjunction of two features. It might be distractors were easy to filter out in the present case because search was accomplished while more than a single visual WM slot was occupied by a target template and further slots had to be kept free to absorb candidate targets (or just features) in view of the target counting task while each MFP sequence was ongoing.

On the other hand, one possibility that cannot be excluded based on the present results is that some form of distractor suppression was at play in ipsilateral ERPs with a lateral target as well as in all three target-absent conditions tested in the present investigation, perhaps as a general reflection of down-weighting colors that could ultimately interfere with the target-color individuation (e.g., Found & Müller, 1996). It is perhaps worth noting in this vein that while potentially distracting colors were used to generate both the heterogeneous and homogeneous target-absent conditions in the present design, the target-absent no-color condition was an exception in this respect, because these displays included only gray circles, that were additionally of lower salience relative to colored circles. In spite of the absence of colored circles in no-color frames, the present results showed that these frames elicited ERP activity that was highly similar to ERPs elicited by heterogeneous and homogeneous frames, making the hypothesis of suppression in all the present baseline conditions unplausible.

As anticipated in the Introduction, ERP studies using visual search typically adopt a subtractive, contralateral-minus-ipsilateral, approach to isolate the N2pc that is blind to bilateral ERP activity that unfolds simultaneously, or after, N2pc. We tend to assume this ERP activity can provide information as important as N2pc for a more thorough understanding of the processing dynamics underlying visual search. To investigate such activity, we explored potential bilateral ERP markers of the processing of selected targets by comparing ERPs elicited by target-present and feature-present frames after subtracting target-absent (heterogeneous) activity, similarly to what was done by Tay et al. (2019, 2022) to isolate the SDP component. Based on the suspect SDP might overlap with other temporally and spatially adjacent ERP components, we carried out an ICA analysis to unmix a prominent positive ERP deflection that, like in Tay et al. (2019, 2022), was in fact detected in target-present minus target-absent ERPs. The ICA analysis of these difference ERPs revealed that two ICA components could be ascribed to unilateral origins (ICA-3 and ICA-6), one ICA component to a bilateral infero-parietal origin (ICA-1), and three ICA components (ICA-2, ICA-4, ICA-5) to bilateral latero-ventral posterior origins. These components were sensitive to the presence of task-relevant features over parieto-occipital scalp areas, similarly to the SDP reported by Tay et al. (2019, 2022). We

observed a positivity when a circle in the target color was present in target-present and feature-present frames after subtracting the ERP recorded in target-absent heterogeneous frames, that were chosen for their physical similarity to the above frames. Differently from Tay et al. (2019, 2022), the time-courses of all four ICA components showed an onset latency that was temporally postponed compared to the N2pc onset, both for feature-present and target-present ICA time-courses.

Of import, after the initial common rise in positivity, the target-present time-course became more positive than the feature-present time-course at different times for all four ICA components. We interpret this initial rise in positivity as an indication the circles in the target color were selected for further processing, which differentiated them clearly from target-absent frames, which did not contain a potential target. Based on the scalp distribution and time-course of ICA-1, we argue ICA-1 was likely to reflect the classic P3b component. One hypothetical caveat concerning the interpretation of ICA-1 as P3b could be that the combined probability of feature-present and target-present frames in the present MFP procedure was higher than that of target-absent frames, the caveat being that P3b is often larger for low-probability events (Donchin, 1981) or for events associated with low-probability overt responses (Dell'Acqua et al., 2005; Sessa et al., 2007). Analogously, considering frames containing a circle in the target color, feature-present frames had the same probability as target-present frames, and P3b should have had an equivalent amplitude in these cases, a scenario which is not in line with the amplitude modulations of target-present and feature-present time-courses discussed so far. On the other hand, ICA-1 responded in a way that was analogous to the P3b amplitude modulation observed by Dell'Acqua et al. (2015) based on target task relevance, and not frequency, in the attentional blink paradigm. A second target embedded in a rapid serial visual presentation stream of distractors elicited a P3b of greater amplitude relative to a non-target in the same position that replaced the target on 50% of trials, a finding that we take as reassuring in relation to our proposal of ICA-1 as candidate activity for P3b.

ICA-2, with a clear focus close to Oz, could be distinguished from P3b based on large differences in scalp distributions. As noted above, the target-present ICA time-course was more positive than the feature-present ICA time-course from about 400 ms to 600 ms post-stimulus, and to almost 800 ms for ICA-4 and ICA-5. The ICA-2 activation might reflect an early portion of PPP and the ICA-5 activation a later PPP portion, with ICA-4 probably arising as an independent combination of these PPP portions. Taken together, we hypothesize that ICA-2, ICA-4, and ICA-5, tracked the visual processing of stimuli selected on the basis of color at different steps in the

information processing flow. The fact PPP activity was not confined to a single ICA component dovetails nicely with this proposal. Contrary to the detection of color, which was likely the feature driving visuo-spatial attention allocation to a possible task-relevant location in the present design, the individuation of a target hinged upon a correct combination of color and bar orientation. Coding color and bar orientation is held to be carried out in distinct neural circuits (e.g., Furmanski & Engel, 2000; Zeki & Marini, 1998). Furthermore, the integration of these two features requires the engagement of visual neurons responding to more abstract stimulus properties, which are hypothesized to be located in infero-temporal (IT) cortical regions (Bar & Biederman, 1999; for ERP evidence, see Keil & Müller, 2010).

Target-present frames differed from feature-present frames also with reference to their different response requirements. As required in the present MFP paradigm, target-present frames had to be processed in terms of incremental count. It is likely that incrementing the internal counter took more time than maintaining the count (which may be achieved by doing nothing, other than preparing for the next stimulus). This specific processing required for target-present frames, reflected in the general increment of PPP activity for target-present relative to feature present frames, could be akin to the SDP amplitude difference between go and no-go trials described by Tay et al. (2022). The go response in our case would correspond to a + 1 count associated with target-present frames, whereas the no-go response would be to skip the counter updating as required by feature-present frames. However, if counter updating had been critical in these respects, ERPs elicited by target-absent heterogeneous frames and feature-present frames should have been undistinguishable, such that there should have been no PPP for the feature-present frames, which was not what we observed in the present results.

In alterative, updating the counter could also be done based on the number of attentional episodes (e.g., Callahan-Flintoft et al., 2018; Wyble et al., 2011; Zivony & Eimer, 2022) that had to be consolidated (Jolicœur & Dell'Acqua, 1998; Ricker & Hardman, 2017; Woodman & Vogel, 2005) in visual working memory for counting purposes. We hypothesize that the PPP may reflect visual attention selection, per se, rather than higher-level cognitive operations required for updating an internal counter upon individuation of a target item (i.e., a specific combination of color circle and bar orientation). A selected target representation would remain active during counter updating, and for a longer time than a representation of just one target feature (i.e., the circle in the target color), as in feature-present frames. This would produce a larger and/or longer PPP for

target-present frames than for feature-present frames. We propose that areas of visual cortex mediating target selection would remain active so as to maintain a link between low-level visual areas and higher-level mechanisms operating on the selected target for counting purposes. In this framework, lower-level visual areas would provide ongoing feedforward support for representations resembling a target. Our hypothesis extends to target-absent frames that did not contain a target-defining feature. As such, the heterogeneous target-absent baseline condition would be most likely to have one or more items selected because of the overall physical similarity of the heterogenous frames with both target-present and feature-present frames. The homogeneous target-absent baseline condition would be less likely to lead to selection (perhaps by spreading rejection after an initial global selection), and the no-color target-absent baseline condition would be the least likely to cause selection, given the absence of color information in those frames. This general framework predicts a decreasing monotonic pattern of PPP amplitudes across the target-absent baseline conditions from heterogeneous, to homogeneous, to no-color frames. This pattern of mean amplitudes is actually visible, in a 400–600 ms time-window, in the ERPs shown in Panel (b) of Figure 2, and a linear contrast on the ERP mean amplitudes recorded at PO7 and PO8 in a 400–600 ms time-window provides good support for this general hypothesis ($F[1, 16] = 7.9$, $\eta_p^2 = .228$, $p = .013$).

Other possible relationships between the PPP in our results and the SDP explored by Tay et al. (2019, 2022) will need to be explored in future research. It is likely that SDP reflected the selection of "pop-out" singleton targets, and as such SDP could be considered a special case of PPP. The present study, however, included numerous differences in procedure, stimulus and search conditions, and methods of analysis compared with Tay's and colleagues. An important difference is that we found the PPP in feature search under conditions that precluded simple pop-out. Furthermore, we provided important new evidence that the PPP reflects more than just the selection of a to-be-attended single feature by tracking the difference, at both the ERP and ICA levels, between target-present and feature-present conditions.

To conclude, both the ipsilateral portion of the N2pc and ERP activity elicited by target-absent visual search arrays appear to be adequate baselines for the computation of the N2pc and the N2pcb. Alternative computations, using ERP activity elicited by target-absent arrays, seem to be a promising tool for the investigation of ERP activity tracking higher-level processing of task-relevant features in visual search, an example of which is the PPP component investigated in the present context.

AUTHOR CONTRIBUTIONS

Roberto Dell'Acqua: Conceptualization; funding acquisition; investigation; methodology; project administration; resources; supervision; visualization; writing – original draft; writing – review and editing. **Mattia Doro:** Conceptualization; data curation; formal analysis; investigation; methodology; writing – original draft; writing – review and editing. **Sabrina Brigadoi:** Investigation; writing – original draft; writing – review and editing. **Brandi Lee Drisdelle:** Data curation; methodology; visualization. **Amour Simal:** Data curation; methodology; visualization. **Valentina Baro:** Investigation; methodology; visualization; writing – review and editing. **Pierre Jolicœur:** Data curation; formal analysis; funding acquisition; investigation; methodology; resources; software; supervision; writing – original draft; writing – review and editing.

ORCID

Roberto Dell'Acqua https://orcid.org/0000-0002-3393-1907
Mattia Doro https://orcid.org/0000-0003-2574-4308
Sabrina Brigadoi https://orcid.org/0000-0003-3032-7381
Amour Simal https://orcid.org/0000-0002-1340-4202
Valentina Baro https://orcid.org/0000-0002-5642-4289

REFERENCES

Arend, A. M., & Zimmer, H. D. (2011). What does ipsilateral delay activity reflect? Inferences from slow potentials in a lateralized visual working memory task. *Journal of Cognitive Neuroscience*, *23*(12), 4048–4056. https://doi.org/10.1162/jocn_a_00068

Aubin, S., & Jolicœur, P. (2016). Early and late selection modulate competition for representation: Evidence from the N2pc in a multiple frame procedure. *Psychophysiology*, *53*(5), 611–622. https://doi.org/10.1111/psyp.12606

Bacigalupo, F., & Luck, S. J. (2019). Lateralized suppression of alpha-band EEG activity as a mechanism of target processing. *Journal of Neuroscience*, *39*(5), 900–917. https://doi.org/10.1523/JNEUROSCI.0183-18.2018

Bacon, W. F., & Egeth, H. E. (1994). Overriding stimulus-driven attentional capture. *Perception & Psychophysics*, *55*(5), 485–496. https://doi.org/10.3758/BF03205306

Bar, M., & Biederman, I. (1999). Localizing the cortical region mediating visual awareness of object identity. *Proceedings of the National Academy of Sciences (USA)*, *96*(4), 1790–1793. https://doi.org/10.1073/pnas.96.4.1790

Benavides-Varela, S., Basso Moro, S., Meconi, F., Brigadoi, S., Doro, M., Simion, F., Sessa, P., Cutini, S., & Dell'Acqua, R. (2018). N2pc reflects two modes for coding the number of visual targets. *Psychophysiology*, *55*(11), e13219. https://doi.org/10.1111/psyp.13219

Benjamini, Y., & Hochberg, Y. (1995). Controlling the false discovery rate: A practical and powerful approach to multiple testing. *Journal of the Royal Statistical Society: Series B (Methodological)*, *57*(1), 289–300. https://doi.org/10.1111/j.2517-6161.1995.tb02031.x

Brisson, B., & Jolicœur, P. (2008). Express attentional re-engagement but delayed entry into consciousness following invalid spatial cues in visual search. *PLoS One*, *3*(12), e3967. https://doi.org/10.1371/journal.pone.0003967

Callahan-Flintoft, C., Chen, H., & Wyble, B. (2018). A hierarchical model of visual processing simulates neural mechanisms underlying reflexive attention. *Journal of Experimental Psychology: General*, *147*(9), 1273–1294. https://doi.org/10.1037/xge0000484.supp

Chen, Y., Brigadoi, S., Schiano Lomoriello, A., Jolicœur, P., Simal, A., Fu, S., Baro, V., & Dell'Acqua, R. (2022). A bilateral SPCN is elicited by to-be-memorized visual stimuli displayed along the vertical midline. *Psychophysiology*, *59*(9), e14045. https://doi.org/10.1111/psyp.14045

Crebolder, J. M., Jolicœur, P., & McIlwaine, J. D. (2002). Loci of signal probability effects and of the attentional blink bottleneck. *Journal of Experimental Psychology: Human Perception and Performance*, *28*(3), 695–716. https://doi.org/10.1037/0096-1523.28.3.695

Dell'Acqua, R., Dux, P. E., Wyble, B., Doro, M., Sessa, P., Meconi, F., & Jolicœur, P. (2015). The attentional blink impairs detection and delays encoding of visual information: Evidence from human electrophysiology. *Journal of Cognitive Neuroscience*, *27*(4), 720–735. https://doi.org/10.1162/jocn_a_00752

Dell'Acqua, R., Jolicœur, P., Vespignani, F., & Toffanin, P. (2005). Central processing overlap modulates P3 latency. *Experimental Brain Research*, *165*(1), 54–68. https://doi.org/10.1007/s00221-005-2281-2

Delorme, A., & Makeig, S. (2004). EEGLAB: An open source toolbox for analysis of single-trial EEG dynamics including independent component analysis. *Journal of Neuroscience Methods*, *134*(1), 9–21. https://doi.org/10.1016/j.jneumeth.2003.10.009

Dien, J., & Frishkoff, G. A. (2005). Principal components analysis of ERP data. In T. C. Handy (Ed.), *Event-related potentials: A methods handbook* (pp. 189–208). Cambridge: MIT Press.

Donchin, E. (1981). Surprise!... Surprise? *Psychophysiology*, *18*(5), 493–513. https://doi.org/10.1111/j.1469-8986.1981.tb01815.x

Doro, M., Bellini, F., Brigadoi, S., Eimer, M., & Dell'Acqua, R. (2020). A bilateral N2pc (N2pcb) component is elicited by search targets displayed on the vertical midline. *Psychophysiology*, *57*(3), e13512. https://doi.org/10.1111/psyp.13512

Drew, T., Mance, I., Horowitz, T. S., Wolfe, J. M., & Vogel, E. K. (2014). A soft handoff of attention between cerebral hemispheres. *Current Biology*, *24*(10), 1133–1137. https://doi.org/10.1016/j.cub.2014.03.054

Drisdelle, B. L., & Eimer, M. (2021). PD components and distractor inhibition in visual search: New evidence for the signal suppression hypothesis. *Psychophysiology*, *58*(9), e13878. https://doi.org/10.1111/psyp.13878

Eimer, M. (1996). The N2pc component as an indicator of attentional selectivity. *Electroencephalography and Clinical Neurophysiology*, *99*(3), 225–234. https://doi.org/10.1016/0013-4694(96)95711-9

Feldmann-Wüstefeld, T., & Schubö, A. (2015). Target discrimination delays attentional benefit for grouped contexts: An ERP study.

Brain Research, *1629*, 196–209. https://doi.org/10.1016/j.brainres.2015.10.018

Feldmann-Wüstefeld, T., & Vogel, E. K. (2019). Neural evidence for the contribution of active suppression during working memory filtering. *Cerebral Cortex*, *29*(2), 529–543. https://doi.org/10.1093/cercor/bhx336

Found, A., & Müller, H. J. (1996). Searching for unknown feature targets on more than one dimension: Investigating a "dimension-weighting" account. *Perception & Psychophysics*, *58*(1), 88–101. https://doi.org/10.3758/BF03205479

Furmanski, C. S., & Engel, S. A. (2000). An oblique effect in human primary visual cortex. *Nature Neuroscience*, *3*(6), 535–536. https://doi.org/10.1038/75702

Gaspar, J. M., Christie, G. J., Prime, D. J., Jolicœur, P., & McDonald, J. J. (2016). Inability to suppress salient distractors predicts low visual working memory capacity. *Proceedings of the National Academy of Sciences*, *113*(13), 3693–3698. https://doi.org/10.1073/pnas.1523471113

Gaspar, J. M., & McDonald, J. J. (2014). Suppression of salient objects prevents distraction in visual search. *Journal of Neuroscience*, *34*(16), 5658–5666. https://doi.org/10.1523/JNEUROSCI.4161-13.2014

Hickey, C., Di Lollo, V., & McDonald, J. J. (2009). Electrophysiological indices of target and distractor processing in visual search. *Journal of Cognitive Neuroscience*, *21*(4), 760–775. https://doi.org/10.1162/jocn.2009.21039

Hubel, D. H., & Wiesel, T. N. (1967). Cortical and callosal connections concerned with the vertical meridian of visual fields in the cat. *Journal of Neurophysiology*, *30*(6), 1561–1573. https://doi.org/10.1152/jn.1967.30.6.1561

Jannati, A., Gaspar, J. M., & McDonald, J. J. (2013). Tracking target and distractor processing in fixed-feature visual search: Evidence from human electrophysiology. *Journal of Experimental Psychology: Human Perception and Performance*, *39*(6), 1713–1730. https://doi.org/10.1037/a0032251

Jolicœur, P., & Dell'Acqua, R. (1998). The demonstration of short-term consolidation. *Cognitive Psychology*, *36*(2), 138–202. https://doi.org/10.1006/cogp.1998.0684

Jolicœur, P., Sessa, P., Dell'Acqua, R., & Robitaille, N. (2006). Attentional control and capture in the attentional blink paradigm: Evidence from human electrophysiology. *European Journal of Cognitive Psychology*, *18*(4), 560–578. https://doi.org/10.1080/09541

Keil, A., & Müller, M. M. (2010). Feature selection in the human brain: Electrophysiological correlates of sensory enhancement and feature integration. *Brain Research*, *1313*, 172–184. https://doi.org/10.1016/j.brainres.2009.12.006

Kiesel, A., Miller, J., Jolicœur, P., & Brisson, B. (2008). Measurement of ERP latency differences: A comparison of single-participant and jackknife-based scoring methods. *Psychophysiology*, *45*(2), 250–274. https://doi.org/10.1111/j.1469-8986.2007.00618.x

Kiss, M., Grubert, A., Petersen, A., & Eimer, M. (2012). Attentional capture by salient distractors during visual search is determined by temporal task demands. *Journal of Cognitive Neuroscience*, *24*(3), 749–759. https://doi.org/10.1162/jocn_a_00127

Lavie, N., Beck, D. M., & Konstantinou, N. (2014). Blinded by the load: Attention, awareness, and the role of perceptual load. *Philosophical Transactions of the Royal Society B: Biological Sciences*, *369*(1641), 20130205. https://doi.org/10.1098/rstb.2013.0205

Lavie, N., Hirst, A., De Fockert, J. W., & Viding, E. (2004). Load theory of selective attention and cognitive control. *Journal of Experimental Psychology: General*, *133*(3), 339–354. https://doi.org/10.1037/0096-3445.133.3.339

Luck, S. J., Fuller, R. L., Braun, E. L., Robinson, B., Summerfelt, A., & Gold, J. M. (2006). The speed of visual attention in schizophrenia: Electrophysiological and behavioral evidence. *Schizophrenia Research*, *85*(1–3), 174–195. https://doi.org/10.1016/j.schres.2006.03.040

Luck, S. J., Girelli, M., McDermott, M. T., & Ford, M. A. (1997). Bridging the gap between monkey neurophysiology and human perception: An ambiguity resolution theory of visual selective attention. *Cognitive Psychology*, *33*(1), 64–87. https://doi.org/10.1006/cogp.1997.0660

Luck, S. J., & Hillyard, S. A. (1994a). Electrophysiological correlates of feature analysis during visual search. *Psychophysiology*, *31*(3), 291–308. https://doi.org/10.1111/j.1469-8986.1994.tb02218.x

Luck, S. J., & Hillyard, S. A. (1994b). Spatial filtering during visual search: Evidence from human electrophysiology. *Journal of Experimental Psychology: Human Perception and Performance*, *20*(5), 1000–1014. https://doi.org/10.1037/0096-1523.20.5.1000

Makeig, S., Jung, T. P., Bell, A. J., Ghahremani, D., & Sejnowski, T. J. (1997). Blind separation of auditory event-related brain responses into independent components. *Proceedings of the National Academy of Sciences (USA)*, *94*(20), 10979–10984. https://doi.org/10.1073/pnas.94.20.10979

Mazza, V., & Caramazza, A. (2011). Temporal brain dynamics of multiple object processing: the flexibility of individuation. *PLoS One*, *6*(2), e17453. https://doi.org/10.1371/journal.pone.0017453

Mazza, V., Turatto, M., & Caramazza, A. (2009). Attention selection, distractor suppression and N2pc. *Cortex*, *45*(7), 879–890. https://doi.org/10.1016/j.cortex.2008.10.009

Monnier, A., Dell'Acqua, R., & Jolicœur, P. (2020). Distilling the distinct contralateral and ipsilateral attentional responses to lateral stimuli and the bilateral response to midline stimuli for upper and lower visual hemifield locations. *Psychophysiology*, *57*(11), e13651. https://doi.org/10.1111/psyp.13651

Morey, R. D., & Rouder, J. N. (2011). Bayes factor approaches for testing interval null hypotheses. *Psychological Methods*, *16*(4), 406–419. https://doi.org/10.1037/a0024377

Nakamura, H., Chaumon, M., Klijn, F., & Innocenti, G. M. (2008). Dynamic properties of the representation of the visual field midline in the visual areas 17 and 18 of the ferret (*Mustela putorius*). *Cerebral Cortex*, *18*(8), 1941–1950. https://doi.org/10.1093/cercor/bhm221

Papaioannou, O., & Luck, S. J. (2020). Effects of eccentricity on the attention-related N2pc component of the event-related potential waveform. *Psychophysiology*, *57*(5), e13532. https://doi.org/10.1111/psyp.13532

Perron, R., Lefebvre, C., Robitaille, N., Brisson, B., Gosselin, F., Arguin, M., & Jolicœur, P. (2009). Attentional and anatomical considerations for the representation of simple stimuli in visual short-term memory: Evidence from human electrophysiology. *Psychological Research*, *73*(2), 222–232. https://doi.org/10.1007/s00426-008-0214-y

Ricker, T. J., & Hardman, K. O. (2017). The nature of short-term consolidation in visual working memory. *Journal of Experimental Psychology: General*, *146*(11), 1551–1573. https://doi.org/10.1037/xge0000346

Sawaki, R., & Luck, S. J. (2010). Capture versus suppression of attention by salient singletons: Electrophysiological evidence for an automatic attend-to-me signal. *Attention, Perception, & Psychophysics*, *72*(6), 1455–1470. https://doi.org/10.3758/APP.72.6.1455

Sessa, P., Luria, R., Verleger, R., & Dell'Acqua, R. (2007). P3 latency shifts in the attentional blink: Further evidence for second target processing postponement. *Brain Research*, *1137*(1), 131–139. https://doi.org/10.1016/j.brainres.2006.12.066

Sharbrough, F., Chatrian, G.-E., Lesser, R. P., Luders, H., Nuwer, M., & Picton, T. W. (1991). American Electroencephalographic Society guidelines for standard electrode position nomenclature. *Journal of Clinical Neurophysiology*, *8*(2), 200–202. https://doi.org/10.1097/00004691-199104000-00007

Simal, A., & Jolicœur, P. (2020). Scanning acoustic short-term memory: Evidence for two subsystems with different time-course and memory strength. *International Journal of Psychophysiology*, *155*, 105–117. https://doi.org/10.1016/j.ijpsycho.2020.06.004

Smulders, F. Y. (2010). Simplifying jackknifing of ERPs and getting more out of it: Retrieving estimates of participants' latencies. *Psychophysiology*, *47*, 387–392. https://doi.org/10.1111/j.1469-8986.2009.00934.x

Tay, D., Harms, V., Hillyard, S. A., & McDonald, J. J. (2019). Electrophysiological correlates of visual singleton detection. *Psychophysiology*, *56*(8), e13375. https://doi.org/10.1111/psyp.13375

Tay, D., Jannati, A., Green, J. J., & McDonald, J. J. (2022). Dynamic inhibitory control prevents salience-driven capture of visual attention. *Journal of Experimental Psychology: Human Perception and Performance*, *48*(1), 37–51. https://doi.org/10.1037/xhp0000972

Van Moorselaar, D., & Slagter, H. A. (2019). Learning what is irrelevant or relevant: Expectations facilitate distractor inhibition and target facilitation through distinct neural mechanisms. *Journal of Neuroscience*, *39*(35), 6953–6967. https://doi.org/10.1523/JNEUROSCI.0593-19.2019

Van Moorselaar, D., & Slagter, H. A. (2020). Inhibition in selective attention. *Annals of the New York Academy of Sciences*, *1464*(1), 204–221. https://doi.org/10.1111/nyas.14304

Vogel, E. K., & Machizawa, M. G. (2004). Neural activity predicts individual differences in visual working memory capacity. *Nature*, *428*(6984), 748–751. https://doi.org/10.1038/nature02447

Wandell, B. A., Dumoulin, S. O., & Brewer, A. A. (2007). Visual field maps in human cortex. *Neuron*, *56*(2), 366–383. https://doi.org/10.1016/j.neuron.2007.10.012

Woodman, G. F., & Vogel, E. K. (2005). Fractionating working memory. *Psychological Science*, *16*(2), 106–113. https://doi.org/10.1111/j.0956-7976.2005.00790.x

Wyble, B., Potter, M. C., Bowman, H., & Nieuwenstein, M. R. (2011). Attentional episodes in visual perception. *Journal of Experimental Psychology: General*, *140*(3), 488–505. https://doi.org/10.1037/a0023612

Zeki, S., & Marini, L. (1998). Three cortical stages of colour processing in the human brain. *Brain*, *121*(9), 1669–1685. https://doi.org/10.1093/brain/121.9.1669

Zeki, S. M. (1993). *A vision of the brain*. Oxford: Blackwell Scientific Publications.

Zivony, A., & Eimer, M. (2022). The diachronic account of attentional selectivity. *Psychonomic Bulletin & Review*. Advance online publication. https://doi.org/10.3758/s13423-021-02023-7